

Experimentally consistent atomistic modeling of bulk and local structure in liquids and disordered materials by empirical potential structure refinement*

Daniel T. Bowron

ISIS Facility, Rutherford Appleton Laboratory, Chilton, Didcot, OX11 0QX, UK

Abstract: This article presents an overview of the use of the empirical potential structure refinement (EPSR) technique for generating three-dimensional atomistic models of liquids and structurally disordered solids that are consistent with experimental neutron and X-ray scattering data. The extension of this technique through the calculation of extended X-ray absorption fine structure (EXAFS) spectra is outlined, and the benefits of this are demonstrated for a range of systems and in particular for our ability to address structural questions of importance in solution chemistry. The model systems chosen as examples for structural analysis are (i) liquid gallium, (ii) silica glass, and (iii) a 1 m aqueous solution of YCl_3 . The advantages of this analytical approach for addressing chemically specific structural questions in disordered systems are discussed within the context of the experimental alternatives based on the techniques of neutron scattering with isotopic substitution and anomalous X-ray scattering.

Keywords: atomistic modeling; neutron scattering; X-ray scattering; EXAFS spectroscopy; solution structure; glass structure.

INTRODUCTION

The detailed mechanisms of in-solution chemical reactions [1] or the materials properties of technological glasses [2] are two examples of current major themes of modern chemistry and physics research. Both problems share the common requirement for chemically specific characterization of the short- and medium-range atomic and molecular structure of structurally disordered media. From the viewpoint of the experimental scientist, some of the most powerful tools available for addressing this issue are neutron and X-ray scattering, and X-ray absorption spectroscopy [3]. The scattering techniques can provide us with detailed information regarding the bulk structural correlations that occur in disordered materials, in particular, the structure of solvent matrices and the atomic or molecular networks that exist in a glass. In contrast, the X-ray absorption spectroscopy techniques provide a powerful chemically specific probe of local structure that can be used to focus a study upon atomic sites that are chemically or physically active, even though these sites may be present at quite high levels of dilution. Though both the scattering and spectroscopy techniques have been available for several decades, it has remained a significant challenge to coherently combine their capabilities within a unified understanding of disordered

*Paper based on a presentation at the 30th International Conference on Solution Chemistry (ICSC 30), 16–20 July 2007, Perth, Australia. Other presentations are published in this issue, pp. 1195–1347.

matter. By and large, research interest has thus either focused on the bulk structure of multicomponent liquids and glasses or on selected local atomic interactions. With the advent of increasingly powerful computational tools and modeling algorithms, it is now beginning to become a realistic possibility to construct comprehensive three-dimensional models of these complex systems that are consistent with available experimental data [4]. These developments thus allow disordered materials researchers to investigate the subtle interplay between detailed aspects of local structural configurations and precisely how these are incorporated into the bulk supporting media.

At the heart of these comprehensive modeling frameworks are reverse modeling algorithms that aim to generate configurations of atoms and molecules that are consistent with available structural data and known physicochemical constraints such as the system's bulk density and the shapes and charge distributions of molecular constituents [4]. The effectiveness of these methods is highly dependent upon the information contained within the data against which they are driven, and in particular for the complex multicomponent systems of general interest, on how unambiguously the various contributions from specific atomic interactions can be identified within the available data sets. This challenge is particularly acute for purely atomic systems where in the absence of the direct measurement of specific interactions between each atom type, there are few other guiding assumptions that can help constrain the resulting structural configurations. Fortunately, for molecular liquids and glasses, the constraints imposed by the system density and the need to pack together known molecular shapes greatly reduces the possible range of structural configurations, and this enhances the possibilities for practical application of the techniques to the study of real chemical systems.

In light of the importance of complementary data to the development of good structural models by these methods, the benefits of being able to combine the results of structural probes with differing sensitivities is immediately apparent. In the following article, we will discuss the use of the empirical potential structure refinement (EPSR) technique [5,6] to build comprehensive three-dimensional models of liquids and disordered solids, with the ultimate view toward the technique's application to questions in structural solution chemistry. Though the technique is designed to work with neutron and X-ray scattering data, we will show the advantages that can now be obtained by combining these models with advanced extended X-ray absorption fine structure (EXAFS) spectroscopy calculations and highlight how this complementary information can greatly enhance our confidence in the resulting models, and also extend the abilities of the technique to address problems that would be ill-constrained by scattering data alone.

METHODS

Empirical potential structure refinement of neutron and X-ray scattering data

At the core of the EPSR method is a Monte Carlo simulation of the structure of an atomic or molecular, liquid, or glass [7]. Conventionally, such simulations are generally parameterized to reproduce some macroscopic thermodynamic quantities of the system of interest such as its phase behavior, but in this case the aim is instead to drive the simulation to reproduce measured structural correlation functions accessible by neutron and X-ray scattering techniques. If a satisfactory model can be built, it can then be interrogated to extract detailed information on site–site interactions that is not directly accessible from the measured correlation functions. Naturally, such models can only be as good as the experimental data against which they are parameterized, and it is therefore beneficial to incorporate as much data in the modeling process as possible. Ideally, each additional data set provides an alternative viewpoint on the structure and better constrains the result. The more unique the data sets to which the model fits, the greater the level of confidence one can have in the result.

Within EPSR, the goal of building an experimentally consistent model is achieved through the generation of interatomic perturbation potentials derived from the experimental data. These are combined with a set of reference potentials, based on Lennard–Jones functions and Coulomb forces [7], that

are used to initialize the model. The simulations themselves make use of Boltzmann-like statistical mechanics methods to generate structural configurations, and as such tend to produce the most disordered models that are consistent with the applied constraints.

The refinement process begins with a standard Monte Carlo simulation of a system of interest performed in the NVT ensemble on a cubic box of atoms and molecules under periodic boundary conditions. Within the starting simulation, the atomic interactions are simply described through the use of Lennard–Jones potentials plus charge interactions. In molecular systems, the configuration of individual molecules is periodically randomized within a simple harmonic spring model to account for their intrinsic zero-point disorder [8]. This procedure is essential as the aim of the simulation is ultimately to produce a model of real experimental data and real systems are not constituted from molecules that are all configurationally identical at any given moment in time. Once the initial simulation has equilibrated, the model is used to generate the correlation functions that can be compared with a neutron or X-ray data set. A difference function is calculated between the model and the experimental structure factor(s), and this difference is used to construct a series of perturbation potentials that are then applied to the reference potentials used to build the model [6]. The simulation is continued under these new potentials, and the process of generating new difference functions and perturbation potentials periodically applied. The process ultimately drives the structural configurations within the simulation box into agreement with the experimental data, and once agreement is reached, the atomic interaction potentials cease to evolve. To follow the evolution of the simulation toward agreement with experimental data, progress can be monitored via an R-factor calculated from the difference between the simulated and experimental structure factors. This tends toward a stable minimum, and once it is achieved, the simulation is considered converged and the Monte Carlo procedure can then be continued so that ensemble average information can be accumulated for structural interrogation. Typically, several million atom moves are required to reasonably reflect the structural configurations that are required to characterize a disordered material such as a liquid or glass.

An important point that must be remembered throughout the structural modeling is that the refinement process is driven by experimental data and this has an often overlooked but important implication, i.e., it is highly unlikely that a simulation will ever produce a *perfect* fit. Experimental data by its very nature will always be subject to a degree of systematic error and statistical uncertainty, and consequently it is important to bear these limitations in mind when evaluating whether an achieved R-factor reflects acceptable convergence.

An advantage of the EPSR technique for disordered materials data analysis is that it allows us to explore the effects of systematic errors in the experimentally derived functions. This can be achieved by noting that the models the process generates are constrained to be consistent with known physical and chemical information, and then by controlling the strength of these constraints in relation to the guiding contributions derived from the experimental data, it is possible to estimate how confident we can be in the quality of the experimental information [6].

Neutron scattering

Given that neutron or X-ray scattering data are the underlying driving force of the modeling process, it is important to understand what information the measured correlation functions impose on the model. In the case of a neutron scattering experiment and following the standard corrections for attenuation and multiple scattering and subtraction of the atomic self scattering, the measured function is the interference differential cross-section or total structure factor $F_N(Q)$ [9]. This is defined in terms of the magnitude of the scattering vector, Q .

$$Q = \frac{4\pi}{\lambda} \sin \theta \quad (1)$$

Here, λ is the wavelength of the incident neutrons and 2θ is the scattering angle. The total structure factor can then be written as

$$F_N(Q) = \sum_{\alpha \leq \beta} (2 - \delta_{\alpha\beta}) c_\alpha c_\beta b_\alpha b_\beta [S_{\alpha\beta}(Q) - 1] \quad (2)$$

This function is a weighted sum of the partial structure factors $S_{\alpha\beta}(Q)$ in terms of the atomic concentrations, c_α and c_β , and neutron scattering lengths, b_α and b_β , of the atoms of type α and β within the sample. To avoid double-counting terms within the summation, $\delta_{\alpha\beta}$ is the Kronecker delta function.

The partial structure factors are the Fourier transforms of the real-space atomic pair distribution functions, $g_{\alpha\beta}(r)$, weighted by the atomic density of the system, ρ :

$$g_{\alpha\beta}(r) - 1 = \frac{1}{(2\pi)^3 \rho} \int_0^\infty 4\pi Q^2 [S_{\alpha\beta}(Q) - 1] \frac{\sin Qr}{Qr} dQ \quad (3)$$

If a single neutron scattering experiment is performed on a sample of interest, then only the total structure factor is obtained and the Fourier transform of this gives the total atomic pair distribution function $g(r)$. This function is often tricky to interpret as many interatomic pair correlations generally occur in similar distance ranges, and consequently their overlap leads to ambiguity in assigning the source of observed features. As a result, it is generally not possible to directly interpret more than the shortest-range structural information contained in a total distribution function, though knowledge of its overall form is important as this provides a stringent defining characteristic of the structure of a disordered material system.

In certain cases, the neutron diffraction technique can be enhanced through the use of isotopic substitution methods [10,11] to directly allow us to access specific pair distribution functions. This is because some elements have isotopes that have markedly different neutron scattering properties. By measuring a series of samples that are assumed to be structurally identical due to having the same chemical composition, but that are isotopically distinct, difference techniques can be used to solve the set of simultaneous equations of $F_N(Q)$, in terms of specific partial structure factors or composite partial structure factors that are more informative than the total [11].

Unfortunately, for complex systems, it is generally not possible to perform enough isotopic series experiments to fully characterize all the site–site interactions. This is due to several reasons: (i) as previously mentioned, suitable isotopes do not exist for every element of the periodic table, (ii) appropriate isotopes of sufficient purity are often extremely difficult to obtain and can be prohibitively expensive, and (iii) preparation of a series of isotopically distinct but structurally identical samples can be a significant challenge, in particular when forming metastable structural systems such as glasses.

X-ray scattering

An alternative to neutron scattering techniques to probe the bulk atomic and molecular structure of a disordered material is X-ray scattering [12]. For X-rays, after corrections for sample absorption, beam polarization, and Compton scattering, the total X-ray differential cross-section measured in an experiment can be expressed as

$$I_X(Q) = \sum_{\alpha} c_{\alpha} f_{\alpha}^2(Q) + \sum_{\alpha \leq \beta} (2 - \delta_{\alpha\beta}) c_{\alpha} c_{\beta} f_{\alpha}(Q) f_{\beta}(Q) S_{\alpha\beta}(Q) \quad (4)$$

where the first term corresponds to the self-scattering from the atomic components in the sample, and the second term to the X-ray interference differential cross-section $F_X(Q)$. $f_{\alpha}(Q)$ and $f_{\beta}(Q)$ are the Q -dependent X-ray scattering form factors that relate the scattering intensity to the atomic number of the el-

ements in the sample in similar fashion to how the Q -independent b_α and b_β relate the neutron scattering intensity in $F_N(Q)$ to the nuclear properties of the elements in the sample.

Following the neutron scattering formalism, $F_X(Q)$ can be extracted by subtracting the single atom scattering contribution to the signal and normalizing the result to the single atom scattering:

$$F_X(Q) = \frac{\left[I_X(Q) - \sum_{\alpha} c_{\alpha} f_{\alpha}^2(Q) \right]}{\sum_{\alpha} c_{\alpha} f_{\alpha}^2(Q)} \quad (5)$$

A comparison of eqs. 2 and 4 illustrates how both the neutron and X-ray scattering measurements essentially probe the same structural information, relating to the pairwise interactions between a sample's constituent atoms. Either of these data sets can thus be used to drive the EPSR process, but the true benefits for the model arise when both sets of information are used together. The difference between the neutron and X-ray scattering weights provides us with independent measures of how the partial structure factors for a system combine to give the total structure factor. Thus, if a model can reproduce both neutron and X-ray data simultaneously, we can have increased confidence in our structural conclusions.

Though this combined use of a single neutron and X-ray experiment cannot provide direct access to a specific pair distribution function in a multicomponent system, X-ray data can be particularly helpful for confirming the structural equivalence of samples in an isotopic series or to provide an additional "effective" isotope in such a series. This is because X-rays only see the chemical composition of a sample reflected through the atomic number of each atom in the sample, which for all isotopic variants is identical. Obviously, the neutron and X-ray combination is also ideal for investigating metastable systems such as glasses, as the same sample can be subject to the two structural probes avoiding any difficulties of having to produce multiple isotopic samples that are structurally identical.

EXAFS modeling

Though the use of neutron scattering with isotopic substitution or combined neutron and X-ray scattering data greatly improves our confidence in models generated by techniques such as EPSR, for many multicomponent systems additional structural information relating specifically to physically and chemically important atomic sites is still required to properly benchmark the quality of the three-dimensional models. In many liquids or disordered solids, the sites of chemical or technological importance are present at relatively high dilution compared to the bulk atomic and molecular constituents, and the scattering methods used to generate the models are consequently insensitive to the details of their environments.

EXAFS spectroscopy is a particularly powerful probe of local atomic structure and is a highly complementary technique to scattering methods. It is a chemically specific probe and in contrast to the scattering experiments discussed above, gives direct access to composite partial structure factors in which all the structural correlations probed must involve the photoexcited atomic species. The method can be applied to the study of the majority of elements in the periodic table and can be used to investigate the local structure around atomic sites present in samples at highly dilute atomic concentrations up to pure element materials. It is therefore potentially highly beneficial to develop the EPSR technique to enable the calculation of EXAFS spectra from the three-dimensional structural models and consequently provide a further means to test the quality of the models against independent partial distribution function sensitive data.

Traditionally, the technique for analyzing EXAFS spectra involves the use of nonlinear curve fitting techniques to parameterize local structural models to experimental data as a series of Gaussian shells of atoms centered on the photoabsorbing atom site [13]. Each shell is characterized by type and

number of neighbors, shell distance, and shell width. Though this is a reasonable approach for the analysis of crystalline samples or disordered systems with a high degree of order in the local environment, this analysis approach is not ideal for the study of highly disordered systems where the distribution of atoms around the photoabsorber is continuous, best characterized by the pair distribution function, and not well represented by a series of discrete shells [14]. This can be seen in eq. 6, which shows the generalized equation for the EXAFS signal in a disordered system, ensemble averaged over structural and dynamic disorder for pair and three-body correlation functions in a monatomic system [15]:

$$\begin{aligned} \langle \chi(k) \rangle = & \int_0^{\infty} 4\pi r^2 \rho g(r) \gamma^{(2)}(r, k) dr \\ & + \int 8\pi^2 r_1^2 r_2^2 \sin(\phi) \rho^2 g_3(r_1, r_2, \phi) \gamma^{(3)}(r_1, r_2, \phi, k) dr_1 dr_2 d\phi \end{aligned} \quad (6)$$

$\gamma^{(2)}$ is the photoelectron scattering signal associated with a single atom located a distance r from the photoabsorber, whilst $\gamma^{(3)}$ is the signal associated with the scattering path involving two atoms located at distances r_1 and r_2 from the photoabsorbing atom and where their position vectors subtend an angle ϕ at this site. The structure in the system is then reflected through the pair distribution function $g(r)$ and the three-body distribution function $g_3(r_1, r_2, \phi)$. Though it is generally true in disordered materials that the contributions to the EXAFS signal are restricted to the leading pair interaction term, for some special cases, the higher-body terms have been found to be significant.

The long-standing challenge for the analysis of EXAFS spectra on highly disordered materials has thus been the incorporation of the continuous and unknown form of the pair distribution function into the analysis framework [14]. The continuous nature $g(r)$ precludes the use of the shell approximation and requires the calculation and averaging of spectral signals and scattering paths for every possible local atomic configuration. This is a computationally intensive problem, but fortunately the advances in modern computing methods now make it a practical possibility to perform these calculations on a reasonable time scale. The classical simulation engines such as incorporated into the EPSR procedure are ideal for this purpose [16].

The essence of the technique is simple. Once the EPSR simulation has converged and the collection of ensemble average structural information is under way, it is a trivial procedure to identify the atomic sites within the model associated with the X-ray absorption edge of interest. Snapshots of the local atomic configurations are then extracted and used to generate the photoelectron scattering potentials, the scattering paths and the resulting EXAFS spectral signals, $\gamma^{(2)}(r, k)$ and $\gamma^{(3)}(r_1, r_2, \phi, k)$, within an advanced spectral calculation code such as the widely used FEFF 8 package [17]. The resulting signals are then ensemble averaged in identical fashion to how other structural functions are extracted from the model, and in this way the functional forms for $g(r)$ and $g_3(r_1, r_2, \phi)$ are intrinsically incorporated into the calculation as they result directly from the ensemble averaging process of the range of local structural configurations sampled. In general, for the cases investigated to date, it has been found that it is necessary to ensemble average several hundred to a few thousand spectral calculations to reasonably capture the range of local structure disorder in the system.

Interestingly, this analysis methodology for EXAFS data avoids the conventional problem of the proliferation of free fitting parameters since all structural EXAFS spectral parameters are fully constrained by the simulation and consequently the neutron or X-ray scattering data against which it is parameterized. This leaves only two unknown parameters in the EXAFS theory that are the magnitude of the energy offset, ΔE_0 , for the spectral energy scale and the magnitude of the amplitude reduction factor, S_0^2 , which is used to account for the multi-electron shake-up and shake-off processes that affect the atomic background, and reduce the magnitude of the EXAFS oscillations [15]. In general, this parameter is typically found to be in the range from 0.7 to 0.9, with L_{III}- and K-edge spectra tending toward the lower and upper limits, respectively. In fact, if the latest theoretical codes for the calculation of EXAFS spectra are utilized (FEFF 8 [17]), the unknown fitting parameters can be further reduced to

one, as it is now possible to theoretically estimate within the latest atomic potential schemes, the likely value of the amplitude reduction factor S_0^2 .

The resulting spectrum produced by the processing of EPSR-derived atomic configurations is thus effectively a direct prediction of the signal that would be expected from the three-dimensional model and its associated set of partial pair distribution functions. It is not a fit to experimental data.

EXAMPLES

The structure of liquid gallium

In his seminal paper of 1972, Narten demonstrated to high precision the equivalence of the neutron and X-ray scattering techniques through a comparison of the structure factors of liquid gallium measured at 20 °C [18]. As this is a monatomic system, the structure factor unambiguously defines the atomic pair distribution function of the liquid, and consequently the data can be used to provide a simple first example of the capabilities of the EPSR technique to build an experimentally consistent three-dimensional model of the system. The structure refinement simulation was performed on a cubic box, 40.1 Å on a side and containing 3375 gallium atoms. Each atom was interacting via a Lennard–Jones potential with values of σ and ϵ set to 2.8 Å and 0.8 kJ mol⁻¹.

Figure 1 shows the EPSR model fit to the neutron and X-ray structure factor of liquid gallium whilst Fig. 2 shows the corresponding pair distribution function and running coordination number. The position of the first peak in $g_{\text{Ga-Ga}}(r)$ tells us that the first-neighbor distance between gallium atoms in this liquid is at 2.76 Å, whilst its integral out to a distance of 3.75 Å tells us that there are ≈ 11.7 neighboring atoms in the first shell. The result confirms the close-packed structure of this liquid metal.

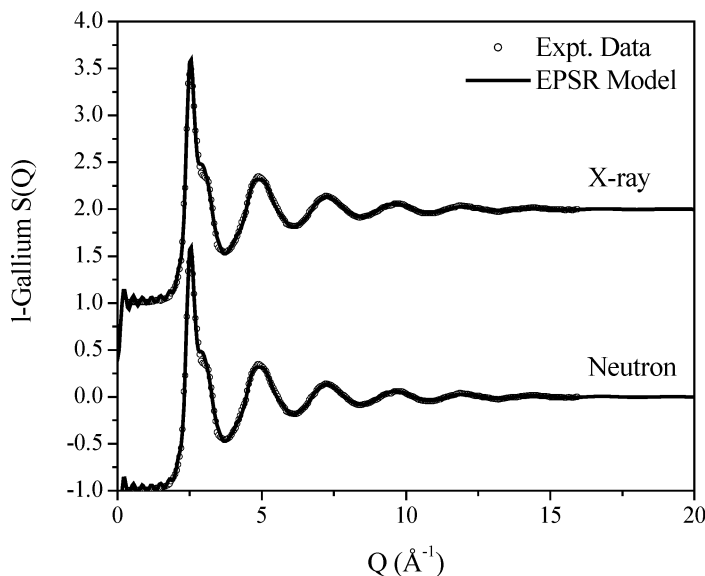


Fig. 1 EPSR model fits to the neutron and X-ray structure factor of liquid gallium at 20 °C [18].

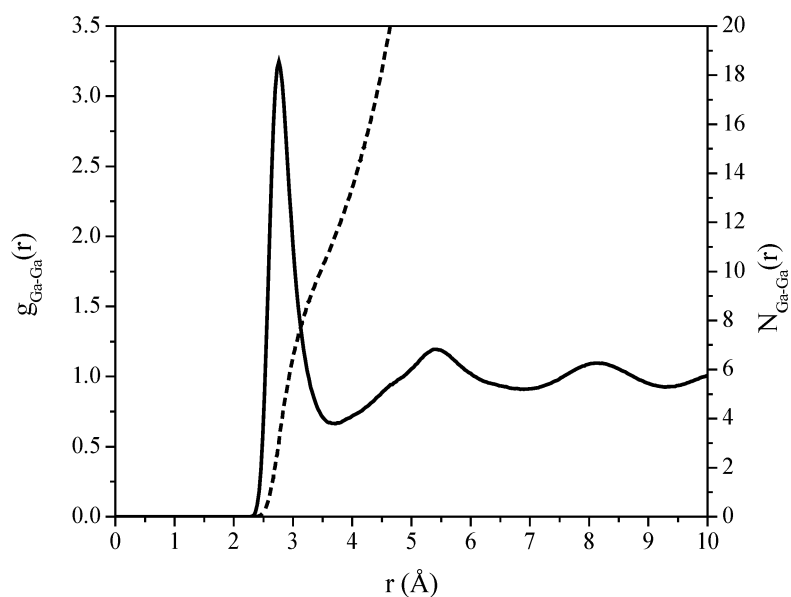


Fig. 2 EPSR-derived pair distribution function and running coordination number for liquid gallium at 20 °C [18].

Noting that Narten's result allowed him to establish the formal equivalence of the neutron and X-ray scattering techniques, this EPSR structural model now allows us to test the capabilities of EXAFS spectroscopy data to be used to corroborate neutron and X-ray scattering derived structural models. Figure 3 shows the liquid gallium EXAFS signal calculated from the three-dimensional EPSR model compared with the experimental result of Comez et al. [19]. Accepting that the comparison is between a model refined against data collected 30 years earlier on a completely independent sample under close but not identical thermal conditions, the comparability of the model to the spectroscopic data is good,

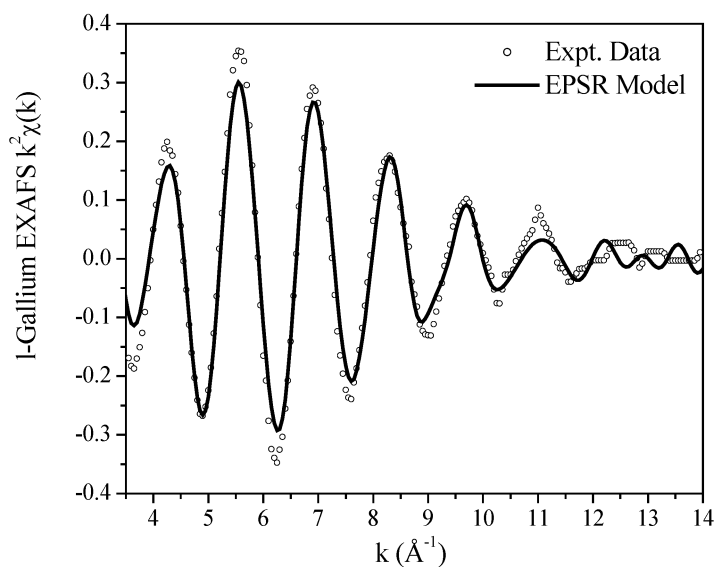


Fig. 3 EPSR-derived EXAFS $k^2\chi(k)$ for liquid gallium at 20 °C, compared with the experimental data of Comez et al. [19] collected at 25 °C.

and certainly comparable to many conventional analyses of EXAFS data that can be found in the literature. Within the model EXAFS calculation, the only parameter varied was the offset of the energy scale within the scattering theory. The optimal value of ΔE_0 was found to be 7 eV. All the structural “parameters” are completely defined by the model, and it is worth also noting that the resulting EXAFS spectrum is fully consistent with the bulk atomic density fluctuations of the liquid captured in the simulation. This is a fundamental constraint that is particularly challenging for conventional EXAFS analysis methods to incorporate robustly as there is no equivalent of the neutron or X-ray scattering structure factor compressibility limit, $S(0)$, for the EXAFS $\chi(k)$ [14].

The structure of silica glass

Moving beyond a monatomic system, the next level of complexity is a binary mixture and silica glass is an ideal system with which to demonstrate the value of a combined neutron and X-ray scattering study. This model will also allow us to show how the results can be further complemented by a comparison with EXAFS spectroscopy data.

As this is a binary system, the structure of the glass requires three partial distribution functions to fully characterize the pairwise interactions between its constituent atoms, namely, $g_{\text{Si-Si}}(r)$, $g_{\text{Si-O}}(r)$, and $g_{\text{O-O}}(r)$. Unfortunately, there are no suitable isotopes of silicon or oxygen that can be used for neutron scattering difference techniques which means that it is not possible to directly extract the three relevant partial structure factors using neutron methods. Only the total neutron structure factor is accessible. In the absence of any other information, any three-dimensional model consistent with these data would not be able to produce an unambiguous separation of the three partial structure functions.

Though X-ray scattering techniques can similarly only allow us to extract a total structure factor, the weightings of the three partial distribution functions from which it is constituted are different from the neutron-weighted experiment. Thus, if the neutron model can reproduce the X-ray data as well, we can have increased confidence in any partial structural conclusions we may draw.

To mimic the behavior of covalent bonding forces in this classical simulation of the glass, the silicon and oxygen atoms were assigned Coulomb charges of $+4e$ and $-2e$ in addition to the Lennard–Jones interactions parameters of $\sigma_{\text{Si}} = 0.76 \text{ \AA}$, $\epsilon_{\text{Si}} = 0.8 \text{ kJ mol}^{-1}$, $\sigma_{\text{O}} = 3.69 \text{ \AA}$, and $\epsilon_{\text{O}} = 0.65 \text{ kJ mol}^{-1}$. Within the simulation, these were combined to calculate the silicon–oxygen interaction using the well-known Lorentz–Berthelot mixing rules [7]. The simulation box consisted of 1000 silicon atoms and 2000 oxygen atoms in a box of side length 35.6 \AA , corresponding to an atomic density of $0.0664 \text{ atoms \AA}^{-3}$.

Figure 4 shows the EPSR model fit and fit residual to the neutron total structure factor for silica glass and also the calculation of the X-ray total structure factor obtained from the model, compared with the seminal X-ray scattering result of Mozzi and Warren [20] on the same system. Clearly, the structural model appears to capture the salient features of both data sets, and this gives us confidence that the simulated three-dimensional structure of the glass is reasonable.

As EXAFS spectra are intrinsically sensitive to a reduced set of the partial structure factors that contribute to the total neutron or X-ray structure factor, this technique can give us considerable further confidence in the quality of our three-dimensional model. If X-ray absorption spectra are collected at the silicon K-edge, the resulting EXAFS $\chi(k)$ contains contributions from $g_{\text{Si-Si}}(r)$ and $g_{\text{Si-O}}(r)$ only, whilst spectra collected at the oxygen K-edge only reflect contributions from $g_{\text{O-O}}(r)$ and $g_{\text{O-Si}}(r)$. For pure silica glass, both sets of experimental data exist in the literature and are available for comparison.

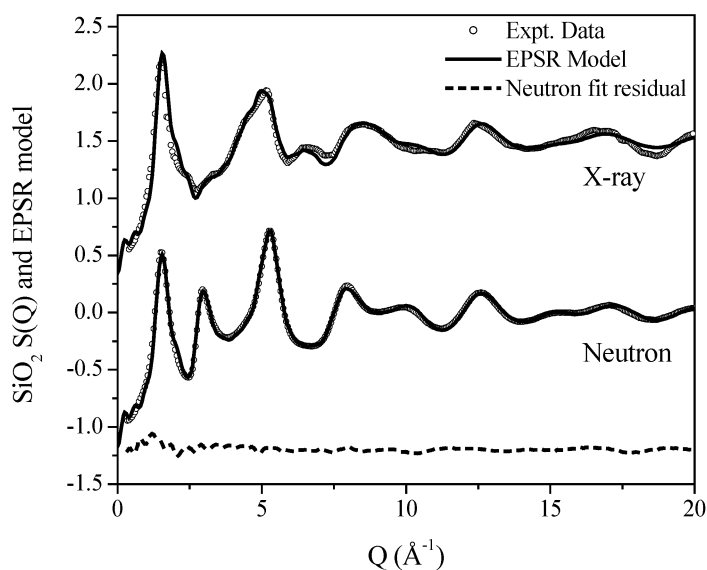


Fig. 4 EPSR model fit and fit residual to the neutron total structure factor data of silica glass at room temperature, and comparison of the X-ray total structure factor calculated from the model with the experimental function measured by Mozzi and Warren [20].

Figure 5 shows the result of the EPSR EXAFS calculation for both absorption edges compared with the experimental data from Greaves et al. for the silicon K-edge [21] and with the data from Stöhr et al. for the oxygen K-edge [22], from which we can conclude that the partial pair distribution functions derived from this model are an acceptable estimate of what are likely to exist in the real glass. It is important to note that current EXAFS theory is generally only accurate for photoelectron energies more than 50 eV above the excitation threshold, and this corresponds to a value of $\approx 3.5 \text{\AA}^{-1}$ for the sig-

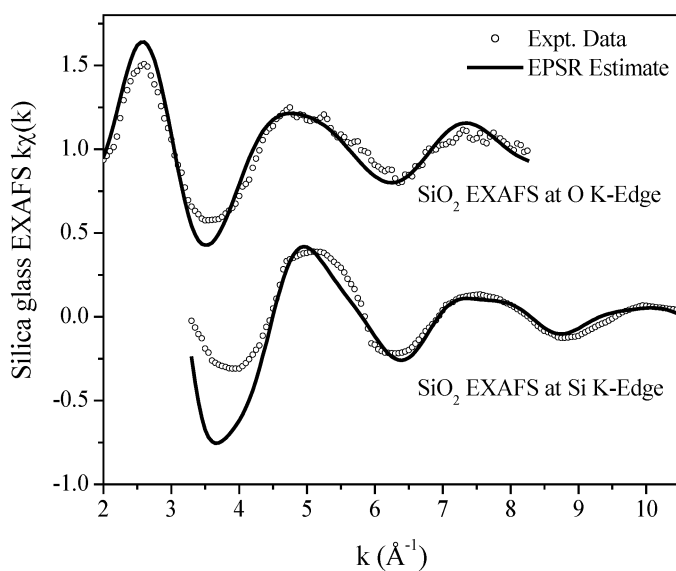


Fig. 5 Comparison of the silicon and oxygen K-edge EXAFS spectra calculated from the neutron data refined model of silica glass with the experimental data of Greaves et al. (Si) [21] and Stöhr et al. (O) [22].

nal in k -space. Below this value, precise details of the atomic potentials that are rarely available, are required to accurately describe the scattering functions, and consequently the misfit in the low- k region of the silicon K-edge spectrum is not unreasonable. For completeness, Fig. 6 shows the three partials in question.

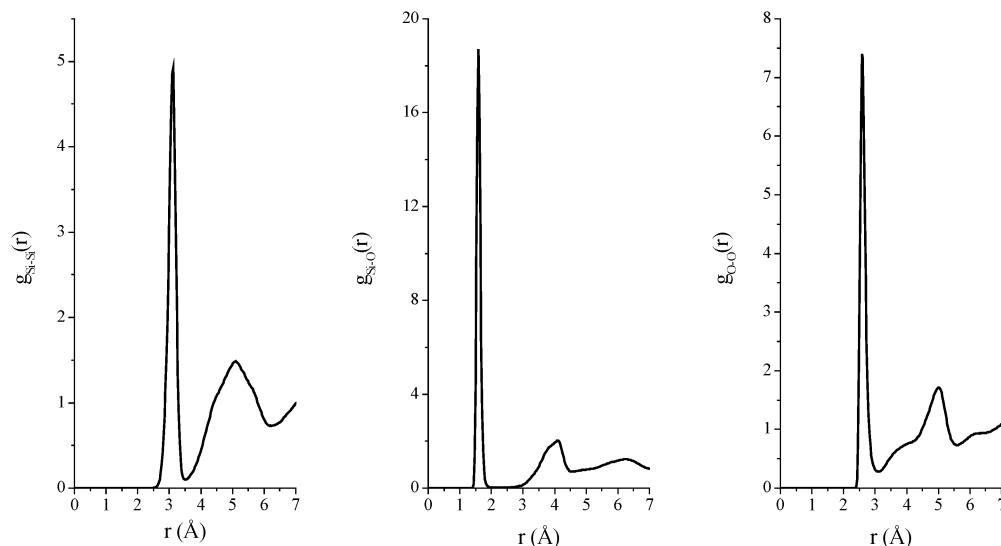


Fig. 6 The silicon–silicon, silicon–oxygen, and oxygen–oxygen pair distribution functions derived from the EPSR model of silica glass that are consistent with neutron scattering, X-ray scattering, and EXAFS spectroscopy data.

Interestingly, it is worth noting that the calculation of the silicon K-edge EXAFS spectrum demonstrated the occasional need to incorporate multiple scattering phenomena in the description of disordered materials EXAFS data. A simple single scattering calculation was unable to account for the asymmetry and widths of the oscillations in the spectrum. The inclusion of three- and four-leg multiple scattering paths within the calculation rectified this difficulty that arose from the significant number of close to colinear Si–O–Si configurations within the glass structure.

The structure of aqueous electrolyte solutions

Determining the structure of aqueous solutions has been a central theme of much of the research undertaken with the EPSR method, and these systems present a further increase in the level of complexity. This is reflected in the number of partial pair distribution functions that are required to fully characterize them. Generally, the equation that defines the number of pair correlations that exist in an n -component atomic system is $n(n + 1) / 2$. For example, in the case of the simple salt solution of 1 m YCl_3 in water, 10 partial distribution functions are required to account for the correlations between the yttrium, chlorine, oxygen, and hydrogen atoms. Specifically, these partials are: $g_{\text{Y-Y}}(r)$, $g_{\text{Y-Cl}}(r)$, $g_{\text{Y-O}}(r)$, $g_{\text{Y-H}}(r)$, $g_{\text{Cl-Cl}}(r)$, $g_{\text{Cl-O}}(r)$, $g_{\text{Cl-H}}(r)$, $g_{\text{O-O}}(r)$, $g_{\text{O-H}}(r)$, and $g_{\text{H-H}}(r)$.

Fortunately, for structural studies of aqueous systems, the neutron scattering technique is particularly powerful as hydrogen/deuterium isotope substitution can be used to gain detailed insight into the intermolecular correlations between water molecules. In pure water, a combination of three H/D isotopic substitution experiments enables us to determine all three partial structure factors that characterize the system, $g_{\text{O-O}}(r)$, $g_{\text{O-H}}(r)$, and $g_{\text{H-H}}(r)$. In aqueous solutions studied by the same technique, the three substitutions enable us to extract $g_{\text{H-H}}(r)$ cleanly, along with two quite informative composite par-

tial structure factors $g_{X-H}(r)$ and $g_{X-X}(r)$, where X signifies all the unlabeled atom types in the mixture [11].

Neutron and X-ray scattering methods are generally most sensitive to the bulk system structure, and dilute species in a solution will only contribute weakly to the measured signals. For example, in the case of a neutron scattering experiment performed on a 1 m solution of YCl_3 in D_2O , the pair correlations involving yttrium ions only contribute to approximately 1.5 % of the total structure factor signal, whilst the correlations involving chloride ions only contribute to a further 5.1 % of the total. The experiment, therefore, is almost completely weighted to the structural correlations involving the water molecules, and any EPSR structure refinement of this data will only weakly be sensitive to the local structural environment of the ions in solution. The resulting model would, therefore, be expected to be a very good representation of the bulk solvent structure, as perturbed by the presence of the ions in solution, but would only reflect the local structure of the ions by virtue of the choice of yttrium and chlorine reference potentials used within the simulation procedure.

Figure 7 shows the EPSR-derived $g_{O-O}(r)$, $g_{O-H}(r)$, and $g_{H-H}(r)$ for a 1 m aqueous solution of YCl_3 [23] compared with the corresponding functions for pure water [24]. The functions were extracted from a model that consisted of 20 Y^{3+} and 60 Cl^- ions along with 1110 water molecules in a cubic box of side length 32.46 Å. Clearly, the presence of ions in the solution has had a marked effect upon the solvent structure, in particular with regards to the water oxygen–oxygen correlations in the distance range from 3 to 6 Å.

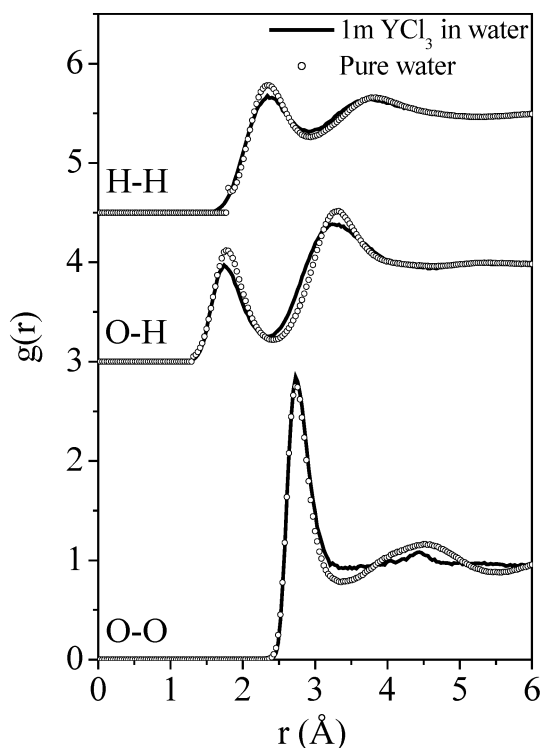


Fig. 7 The water oxygen and hydrogen partial pair distribution functions, $g_{O-O}(r)$, $g_{O-H}(r)$, and $g_{H-H}(r)$, derived from an EPSR model of 1 m YCl_3 in water [23] compared with the equivalent functions for the pure solvent [24].

In contrast to the scattering experiments, EXAFS spectroscopy is highly sensitive to dilute species. It is thus easy to see how the availability of EXAFS data centered on the ion sites could now be used to test how well the reference potentials for the ionic species in the simulation capture the local structure of their environments. Subsequently, it is possible to assess how comprehensively the three-dimensional model reproduces the overall structure of the solvent system [23].

Figure 8 shows the calculated yttrium K-edge EXAFS spectrum extracted from the EPSR simulation and obtained for two choices of the Lennard–Jones interaction potential used to describe the Y^{3+} cation within the model, compared with the experimental data of Díaz-Moreno et al. [25]. The first model defines σ_Y as 3.25 Å, whilst the second model defines σ_Y as 3.1 Å. When combined with the SPC/E parameters [26] used to describe the water molecules within the EPSR simulation, these two choices of σ lead to average Y^{3+} –O distances of 2.39 and 2.33 Å, respectively. Due to the fact that the yttrium–oxygen correlation only makes approximately a 0.4 % contribution to the neutron total structure factors used to refine the model, this change in the reference potential makes no difference to the overall quality of the EPSR fit to the scattering data. In contrast, Fig. 8 shows the consequences for the simulation of the EXAFS signal are significant. Figure 9 shows the yttrium–oxygen pair distribution function that is consistent with the optimized potential structure refinement.

The incorporation of the EXAFS calculation into this study of an aqueous electrolyte solution is thus a very valuable advance. The ability to test a local structural conclusion drawn from a bulk sensitive neutron scattering-based model against an independent measurement has enabled us (i) to obtain useful insight into the failings of an atomic interaction potential, (ii) to refine our choice of an optimum potential, and (iii) subsequently to develop a model that is consistent with both the bulk solution structure and the local environment of the cations in solution.

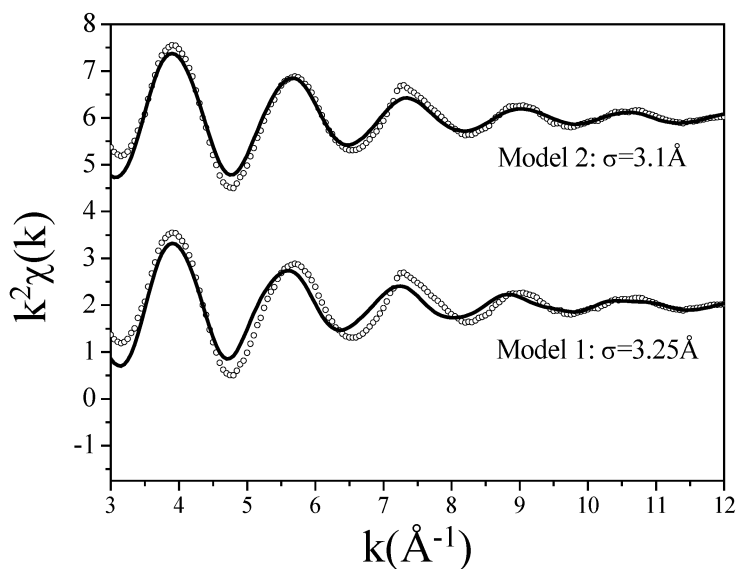


Fig. 8 EPSR-derived Y K-edge EXAFS for a 1 m aqueous solution of YCl_3 compared with experimental data of Díaz-Moreno et al. [25]. The figure illustrates the effect of the choice of σ used for the Lennard–Jones reference potential that describes the Y^{3+} interactions within the EPSR simulation.

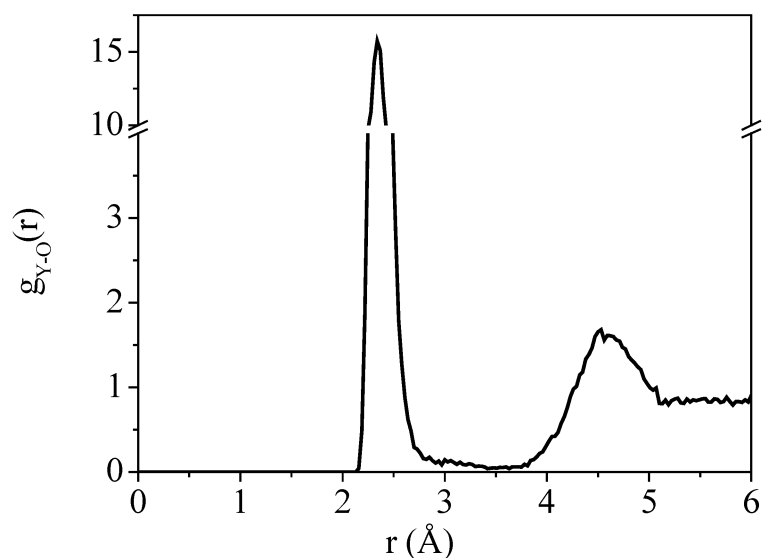


Fig. 9 The yttrium–oxygen pair distribution function $g_{Y-O}(r)$ consistent with the optimized potential refinement of the 1 m aqueous solution of YCl_3 .

The availability of a full three-dimensional model of the solution is now particularly advantageous, as it is then a trivial matter to extract detailed information on subtle structural aspects such as the geometry of the ion hydration shells. Figure 10 shows the O–Y–O first neighbor bond angle distribution extracted from the refined structural model. The dominant angle correlations are clearly centered at 72° and 141° , which are consistent with a local hydration shell geometry formed by eight water molecules distributed around the Y^{3+} cation, arranged at the corners of a square antiprism [25,27].

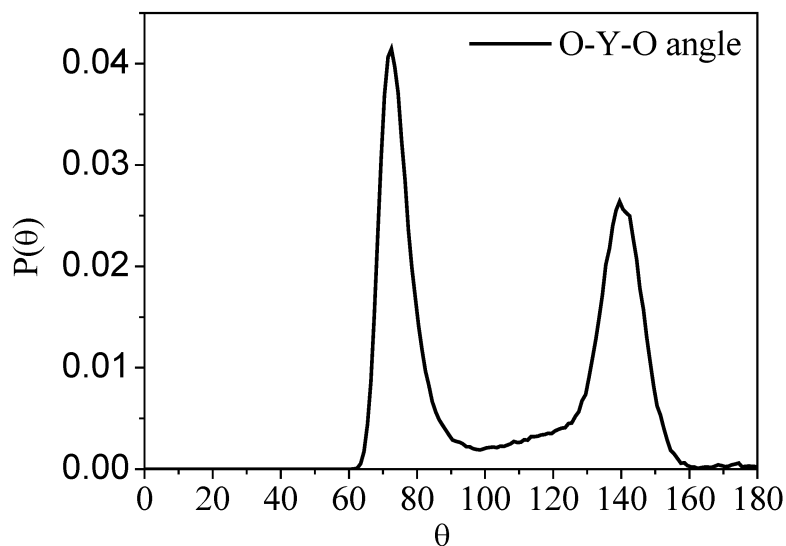


Fig. 10 The first neighbor O–Y–O bond angle distribution extracted from the EPSR-refined model. The peaks at 72° and 141° are consistent with the local geometry of the Y^{3+} cation, adopting the form of a square antiprism.

A central chemical issue that it is important to address for ions in solution is the range and types of hydrated ion species present in solution under various conditions. The described analytical approach provides us with the potential to investigate the likely partitioning of differing hydrated species. For hydrated cations such as Y^{3+} where the residence time of a water molecule in the first hydration shell is short, the described model based simply on water, cations, and anions constrained within the simulation box is likely to produce a reasonable estimate of the range of hydrated ion species likely to exist at any given time [23]. In more complex cases such as the hydration of Cr^{3+} , where the cation is known to be strongly solvated by six water molecules in its first hydration shell and where each molecule has a very long residence time, it is necessary to incorporate this information into the initial simulation. One way that this can be achieved is through the introduction into the model of a $[Cr \cdot 6H_2O]^{3+}$ molecular complex instead of Cr^{3+} , which avoids the tendency of the Monte Carlo simulation method to overly disorder the local structural environment of the cation. EXAFS data would at this point be particularly useful as it would allow the model of the molecular ion incorporated into the simulation to be checked for whether it reasonably reflects the local structure around the cation itself.

DISCUSSION AND CONCLUSIONS

The ultimate aim of the EPSR procedure is the production of an accurate three-dimensional representation of the atomic and molecular structure in a disordered material or liquid. Within this quest, the only means available to the experimental scientist to establish the veracity of any model is through a comparison with available experimental data. The above examples show, in systems of increasing structural complexity, the immense value of combining local structural information obtained using X-ray absorption spectroscopy techniques into the refinement of three-dimensional structural models from neutron and X-ray scattering data. The unique characteristics of this spectroscopy that greatly complement the scattering experiments are (i) its intrinsic chemical selectivity giving direct access to composite partial structure factor information as opposed to the total structure factor, (ii) its sensitivity to dilute atomic components that only make small contributions to the scattering experiment signals, (iii) its sensitivity to the details of the short-range interatomic potentials, and (iv) its wide applicability to almost all the elements of the periodic table.

The ability to obtain chemically specific information from almost the whole periodic table of elements is an exceptional advantage. By scattering techniques, chemically specific access to individual partial distribution functions or composite partial distribution functions is only achievable through the use of neutron scattering isotopic substitution methods or by the fiendishly difficult anomalous X-ray scattering method [28]. The neutron scattering techniques are intrinsically limited to elements that have isotopes with sufficiently different neutron scattering lengths to enable a measurable difference in the scattering signals observed from two or more structurally identical but isotopically distinct samples. Hydrogen and deuterium are perhaps the most celebrated isotopes suitable for this kind of work, but they are unusual in that they are relatively easy to obtain for a reasonable cost. For most other elements where the substitution technique is a possibility, obtaining isotopes of sufficient purity and furthermore using them to fabricate sufficient quantities of sample for investigation is a significant challenge. These difficulties inevitably lead to often prohibitive costs.

Though applicable to a larger fraction of the elements, the anomalous X-ray scattering technique only starts to become feasible for elements heavier than copper if atomic resolution is required of the scattering data, and then it still remains a significant challenge to correct such data for unavoidable parasitic contributions to the structural signal with sufficient accuracy for a reliable structure determination [29].

As both these specialized neutron and X-ray methods are scattering-based, they also require a significant fraction of the sample to consist of the element whose local structure is to be probed. The minimum is typically in the region of 1–10 % of the total number of atoms. Furthermore, to obtain data of

sufficient statistical quality to permit partial structure factor analysis, long data collection times, in the range of hours to days, are generally required.

In contrast, the EXAFS technique is simple to apply to structurally disordered systems and highly sensitive to dilute quantities of any element of interest. With the expansion in the availability of synchrotron radiation sources, this technique is also becoming increasingly easy to access. As no special sample preparation requirements are generally needed and the time required for the experiments to be performed is short (on the order of minutes), the costs for such studies are comparatively low. The traditional difficulties that have plagued the extraction of structural information from the data, and that have previously tarnished the general perception of this technique, are primarily an artefact of the available analysis methodologies. In the conventional approach, many model parameters are generally required to describe a spectral signal obtained in a finite range and with limited accuracy. By avoiding direct fitting of the EXAFS data, the methods outlined here allow us to remove the problem of parameter proliferation. The spectral data are simply used as an independent and unique fingerprint against which the predictions of a scattering data-based model can be tested. By this approach, it is possible to bring dilute component sensitivity to bulk structure models and to refine the short-range atomic potentials to which the spectral data are highly sensitive.

The benefits of this comprehensive data analysis scheme are thus manifold, and this approach now opens a path by which previously intractable structural problems of central chemical and technological importance may be coherently addressed. The method allows us to simultaneously investigate on both short- and intermediate-length scales and at realistic sample compositions, complex multicomponent systems. Examples where immediate advances may now be made include the investigation of the detailed interplay between local ion solvation structures and bulk solvent interactions at realistic reaction concentrations, and the short- and intermediate-range structural interactions of photoactive atomic species embedded in technologically important silicate and phosphate glasses.

REFERENCES

1. E. Buncel, R. Stairs, H. Wilson. *The Role of the Solvent in Chemical Reactions*, Oxford University Press, Oxford (2003).
2. A. J. Ikushima, T. Fujiwara, K. Saito. *Appl. Phys. Rev.* **88**, 1201 (2000).
3. N. E. Cusack. *The Physics of Structurally Disordered Matter*, Adam Hilger, Bristol (1987).
4. R. L. McGreevy. *J. Phys. Condens. Matter* **13**, R877 (2001).
5. A. K. Soper. *Chem. Phys.* **202**, 298 (1996).
6. A. K. Soper. *Phys. Rev. B* **72**, 104204 (2005).
7. M. P. Allen, D. J. Tildesley. *Computer Simulation of Liquids*, Clarendon Press, Oxford (1987).
8. A. K. Soper. *Mol. Phys.* **99**, 1503 (2001).
9. A. K. Soper, W. S. Howells, A. C. Hannon. *ATLAS – Analysis of Time-of-Flight Diffraction Data from Liquid and Amorphous Samples*; Rutherford Appleton Laboratory Report, RAL 89-046 (1989).
10. J. E. Enderby, D. M. North, P. A. Egelstaff. *Philos. Mag.* **14**, 961 (1966).
11. J. L. Finney, A. K. Soper. *Chem. Soc. Rev.* **23**, 1 (1994).
12. B. E. Warren. *X-ray Diffraction*, Dover, New York (1990).
13. A. Filipponi, A. Di Cicco, C. R. Natoli. *Phys. Rev. B* **52**, 15122 (1995).
14. A. Filipponi. *J. Phys. Condens. Matter* **6**, 8415 (1994).
15. A. Filipponi. *J. Phys. Condens. Matter* **13**, R23 (2001).
16. G. Ferlat, J.-C. Soetens, A. San Miguel, P. A. Bopp. *J. Phys. Condens. Matter* **17**, S145 (2005).
17. A. L. Ankudinov, B. Ravel, J. J. Rehr, S. D. Conradson. *Phys. Rev. B* **58**, 7565 (1998).
18. A. H. Narten. *J. Chem. Phys.* **56**, 1185 (1972).
19. L. Comez, A. Di Cicco, J.-P. Itié, A. Polian. *Phys. Rev. B* **65**, 014114 (2001).
20. R. L. Mozzi, B. E. Warren. *J. Appl. Crystallogr.* **2**, 164 (1969).

21. G. N. Greaves, A. Fontaine, P. Lagarde, D. Raoux, S. J. Gurman. *Nature* **293**, 611 (1981).
22. J. Stöhr, L. Johansson, I. Lindau, P. Pianetta. *Phys. Rev. B* **20**, 664 (1979).
23. D. T. Bowron, S. Díaz-Moreno. *J. Phys. Chem. B* **111**, 11397 (2007).
24. A. K. Soper. *Chem. Phys.* **258**, 121 (2000).
25. S. Díaz-Moreno, A. Muñoz-Paez, J. Chaboy. *J. Phys. Chem. A* **104**, 1278 (2000).
26. H. J. C. Berendsen, J. R. Grigera, T. P. Straatsma. *J. Phys. Chem.* **91**, 6269 (1987).
27. T. Ikeda, M. Hirata, T. Kimura. *J. Chem. Phys.* **122**, 024510 (2005).
28. P. H. Fuoss, P. Eisenberger, W. K. Warburton, A. Bienenstock. *Phys. Rev. Lett.* **46**, 1537 (1981).
29. S. Ramos. “Resonant X-ray Scattering Studies of Concentrated Aqueous Solutions”, Ph.D. thesis, University of Bristol, UK (2001).